of or extensive deposition on the sampler and skimmer (8) are readily removed by this technique. Some important analyte metals are not complexed strongly by DTC under the conditions used in the present work. With small changes in conditions or in the complexing group itself, other metals such as Zn, Cd, Pb, and U can likely be preconcentrated by this method. The preconcentration and separation abilities of this procedure should be useful for the analysis of seawater and other highly saline samples such as digested biological tissues, brines, fluid inclusions in minerals, and the dissolved melts resulting from high-temperature fusions (e.g., with lithium metaborate or sodium carbonate).

LITERATURE CITED

(1) Houk, R. S.; Fassel, V. A.; Flesch, G. D.; Svec, H. J.; Gray, A. L.; Taylor, C. E. *Anal. Chem.* **1980**, *52*, 2283–2289.
(2) Houk, R. S.; Thompson, J. J. *Mass Spectrom. Rev.* **1988**, *7*, 425–462.
(3) Houk, R. S. *Anal. Chem.* **1986**, *58*, 97A–105A.
(4) Douglas, D. J.; Houk, R. S. *Prog. Anal. At. Spectrosc.* **1985**, *8*, 1–18.
(5) Tan, S. H.; Horlick, G. *Appl. Spectrosc.* **1986**, *40*, 445–460.
(6) Tan, S. H.; Horlick, G. *J. Anal. At. Spectrom.* **1987**, *2*, 745–763.
(7) Olivares, J. A.; Houk, R. S. *Anal. Chem.* **1986**, *58*, 20–25.
(8) Douglas, D. J.; Kerr, L. A. *J. Anal. At. Spectrom.* **1988**, *3*, 749–752.
(9) Dean, J. D.; Massey, R.; Ebdon, L. J. *J. Anal. At. Spectrom.* **1987**, *2*, 369–374.
(10) McLaren, J. W.; Mykytiuk, A. P.; Willie, S. N.; Berman, S. S. *Anal. Chem.* **1985**, *57*, 2907–2911.
(11) Beauchemin, D.; McLaren, J. W.; Mykytiuk, A. P.; Berman, S. S. *Anal. Chem.* **1987**, *59*, 778–783.
(12) Thompson, J. J.; Houk, R. S. *Appl. Spectrosc.* **1987**, *41*, 801–806.
(13) Beauchemin, D.; McLaren, J. W.; Berman, S. S. *Spectrochim. Acta, Part B* **1987**, *42B*, 467–490.
(14) Beauchemin, D.; McLaren, J. W.; Mykytiuk, A. P.; Berman, S. S. *J. Anal. At. Spectrom.* **1988**, *3*, 305–308.
(15) McLaren, J. W.; Beauchemin, D.; Berman, S. S. *J. Anal. At. Spectrom.* **1987**, *2*, 277–281.
(16) McLeod, C. W.; Date, A. R.; Cheung, Y. Y. *Spectrochim. Acta, Part B* **1986**, *41B*, 169–174.
(17) Date, A. R.; Cheung, Y. Y.; Stuart, M. E. *Spectrochim. Acta, Part B* **1987**, *42B*, 3–20.
(18) Lichte, F. A.; Meier, A. L.; Crock, J. G. *Anal. Chem.* **1987**, *59*, 1150–1157.
(19) Pruszkowski, E.; Ediger, R.; Carnrick, G.; Voelkopf, U. *At. Spectrosc.*, in press.
(20) Park, C. J.; Van Loon, J. C.; Arrowsmith, P.; French, J. B. *Anal. Chem.* **1987**, *59*, 2191–2196.
(21) Beauchemin, D.; Berman, S. S., submitted for publication in *Anal. Chem.*
(22) Lyon, T. D. B.; Fell, G. S.; Hutton, R. C.; Eaton, A. N. *J. Anal. At. Spectrom.* **1988**, *3*, 601–603.
(23) Palmieri, M. D.; Fritz, J. S.; Thompson, J. J.; Houk, R. S. *Anal. Chim. Acta* **1986**, *184*, 187–196.
(24) Jiang, S.-J.; Palmieri, M. D.; Fritz, J. S.; Houk, R. S. *Anal. Chim. Acta* **1987**, *200*, 559–571.
(25) Hulanicki, A. *Chem. Anal.* **1966**, *11*, 1081.
(26) Olson, K. W.; Haas, W. J., Jr.; Fassel, V. A. *Anal. Chem.* **1977**, *49*, 632–637.
(27) Bear, B. R.; Fassel, V. A. *Spectrochim. Acta, Part B* **1986**, *41B*, 1089–1113.
(28) Scott, R. H.; Fassel, V. A.; Kniseley, R. N.; Nixon, D. E. *Anal. Chem.* **1974**, *46*, 75–80.
(29) Junk, G. A.; Richard, J. J.; Grieser, M. D.; Witiak, D.; Witiak, J. L.; Arguello, M. D.; Vick, R.; Svec, H. J.; Fritz, J. S.; Calder, G. V. *J. Chromatogr.* **1974**, *99*, 745–762.
(30) Jones, M. M.; Burka, L. T.; Hunter, M. E.; Basinger, M.; Campo, G.; Weaver, A. D. *J. Inorg. Nucl. Chem.* **1980**, *42*, 775–778.
(31) Galus, M.; Hulanicki, A. *Chem. Anal.* **1972**, *17*, 739–744.
(32) Plantz, M. R. M.S. Dissertation, Iowa State University, 1988.
(33) Munder, H. A. Ph.D. Dissertation, University of Ulm, 1987; p 50.
(34) Cotton, F. A.; Wilkinson, G. Advanced Inorganic Chemistry, 4th ed.; Wiley-Interscience: New York, 1980; p 716.

RECEIVED for review July 25, 1988. Accepted October 18, 1988. This paper was presented in part at the Spring Symposium of the Minnesota Chromatography Forum, Minneapolis, MN, 1988. Ames Laboratory is operated for the U.S. Department of Energy by Iowa State University under Contract No. W-7405-ENG-82. This research was supported by the Director of Energy Research, Office of Basic Energy Sciences.

Evaluation of Pulsed Fast-Atom Bombardment Ionization for Increased Sensitivity of Tandem Mass Spectrometry

R. E. Tecklenburg, Jr., M. E. Castro, and D. H. Russell*

Department of Chemistry, Texas A&M University, College Station, Texas 77840

The use of pulsed valves for performing fast-atom bombardment (FAB) ionization on a sector ion-beam mass spectrometer is described. The objective of this work is to establish new methods for improving the sensitivity of tandem mass spectrometry. This paper deals with the use of pulsed FAB for improving total ion yields as well as signal-to-noise ratios for collision-induced dissociation and laser-ion beam photodissociation. Pulsing the neutral gas pressure used for FAB ionization results in neutral primary beam densities much greater (by a factor of 10) than those obtainable for continuous FAB. This approach yields enhancements for total ion yields and collision-induced dissociation signals by a factor of 15, while larger gains (>28) are measured for the comparable photodissociation experiment.

INTRODUCTION

Since the introduction of fast-atom bombardment (FAB) ionization (*1*, *2*), fast-atom bombardment mass spectrometry (FAB-MS) of large molecules has become almost routine (*3*, *4*). Tandem mass spectrometers equipped with FAB ionization sources are frequently used for the sequencing of polypeptides as well as structure elucidation of large biomolecules (*5–9*). Unlike the more conventional ionization methods such as electron impact and chemical ionization which produce ion currents in the range 10^{-9}–10^{-10} A, ion currents from fast-atom bombardment are typically 3 orders of magnitude smaller and rapidly decrease as a function of the molecular weight of the sample. Although the new generation of high-performance mass spectrometers is capable of performing mass analysis on high mass ions (m/z 5000–15000), the ability to produce sufficient numbers of ions for detailed structural characterization (e.g., collision-induced dissociation (CID) and/or photodissociation) is presently a limitation. A second disadvantage of FAB ionization for use with tandem mass spectrometry is that the mass spectra are noisy (in terms of chemical noise), thus limiting the advantages of signal-to-noise enhancement by using signal-averaging methods. In addition, sample lifetimes are relatively short (10–20 min), and this also

0003-2700/89/0361-0153$01.50/0

limits the use of signal averaging to enhance the signal-to-noise ratios for CID or photodissociation spectra.

In order to fully realize the potential of FAB-MS, and especially the combined use of FAB and tandem mass spectrometry for structural characterization of large molecules, increased sensitivity must be obtained. Although there are potentially two areas where the sensitivity of FAB tandem mass spectrometry can be enhanced, e.g., ionization efficiency and more efficient conversion of the $[M + H]^+$ or $[M - H]^-$ ion to structurally significant fragment ions, this paper addresses the sensitivity enhancement related to the absolute yield for secondary ions per unit concentration of the analyte (*10*). Although problems (signal-to-noise enhancement by using signal averaging) related to the rate of sample consumption can be negated by the use of flow FAB, and improvements in the "signal-to-chemical noise ratio" have been documented for flow FAB (*11*), there are no intrinsic sensitivity gains realized by this method of sample introduction.

A recent paper by Hunt et al. using a pulsed (4 ms, 200 Hz) Cs^+ ion source suggests that ion yields for 100–200 pmol quantities of oligopeptides and small proteins are larger than those obtained by continuous FAB (*12*). For example, Cs^+ ion bombardment of a liquid matrix containing 100–200 pmol of bovine and porcine insulin or horse cytochrome *c* produced ample numbers of ions for detection by Fourier transform ion cyclotron resonance (FT-ICR). There are insufficient details on the tandem quadrupole FT-ICR apparatus (specifically the efficiency of transport of ions from the ion source to the ICR ion trap cell and the efficiency for trapping the ions) to measure absolute numbers of ions contributing to a given signal; however, we were surprised that such excellent signal-to-noise ratios could be obtained for large molecules with such relative ease. Our own experience also suggests that increased sensitivities can be obtained by using pulsed secondary ion mass spectrometry (SIMS) type ion sources (*13*). These results motivated us to examine more carefully the details of the experiment. Specifically, there are several factors that could lead to increased sensitivity for pulsed Cs^+ SIMS over continuous FAB: (i) The increased ionization efficiency of a pulsed Cs^+ ion gun over neutral continuous FAB ionization may in part be due to the fact the Cs^+ ion beam can be directed and focused to a small spot size relative to the dimensions of the probe tip (*14*). (ii) The negligible gas load that the Cs^+ ion gun adds to the ion source region is another advantage and may lead to increased ion yields over continuous FAB guns. This idea is supported by recent work by Aberth which demonstrates that the ion currents of large molecular weight cesium ion clusters are strongly attenuated at high ion source pressures ($>2 \times 10^{-7}$ Torr) (15). (iii) The secondary ion optics for most Cs^+ SIMS instruments have been designed specifically for that purpose, whereas most FAB ion sources are modified versions of sources designed for other (e.g., electron impact ionization) purposes. Thus, in order to make direct comparisons between continuous and pulsed FAB it is essential to do just that, i.e., make direct comparisons between the two modes (pulsed and continuous) of operating a FAB source.

Olthoff and Cotter have performed pulsed liquid SIMS (primary ions, Xe^+) on a series of peptides and large biomolecules and found that the high primary ion current densities (up to 150 $\mu A/cm^2$) achievable with the pulsed gun resulted in high secondary ion yields (*16*). The authors also noted an attenuation in the secondary ion yields with increasing repetition rate of the pulsed gun and rationalized this result in terms of a finite time required to repair damage to the sputtered liquid surface.

The use of pulsed ionization with a scanning magnetic sector mass spectrometer may appear as an unnatural combination. For instance, as the magnetic field strength is scanned to record the mass spectrum, the ion beam is projected onto a slit and ions that pass through the slit strike the detector and produce the ion signal. The complication in using a pulsed ionization source arises as a result of scanning the magnet and projecting the ions onto the slit; if a particular m/z value is projected onto the slit when the ionization is in the "off" cycle, no ions are detected. Thus, to record a mass spectrum the pulse rate of the ionizing radiation must be fast relative to the scan rate. However, experiments such as photodissociation are well suited for pulsed ionization. Also, it is quite resonable to perform collision-induced dissociation in conjunction with pulsed ionization, especially on instruments where MS-II is an electrostatic analyzer (relatively broad signals with poor m/z resolutions) or if detection is performed by using an array detector or a time-of-flight analyzer. Thus, there exist specialized experiments for magnetic sector instruments where pulsed ionization is compatible and may even have particular advantages, especially if one can use these methods to enhance sensitivity.

The sensitivity (secondary ion yield per analyte concentration unit) of the saddle field gun used for continuous FAB ionization can be increased by operating the gun at higher neutral flux (>10–20 μA), but this tends to exacerbate the sample lifetime problem, attenuate the ion signals (due to increased source pressures), and quickly reduce the efficiency of the FAB gun. Another problem with continuous FAB ionization is that the fast-neutral beam is broad and unfocused, which results in only a small fraction of the fast-neutral beam striking the FAB probe tip. In this paper we compare and quantify collision-induced dissociation, photodissociation, and ionization yields for both pulsed and continuous fast-atom bombardment ionization.

EXPERIMENTAL SECTION

The results presented here were obtained with a Kratos MS-50TA instrument. The mass spectrometer has been described in detail in an earlier paper (*17*). Ion detection can be performed by a standard off-axis postacceleration detector or by an on-axis 16-stage Hamamatsu R515 electron multiplier and an EG&G Ortec ion counting system. The on-axis electron multiplier and ion counting were used for the studies reported here. The ion counting apparatus consists of a Model 9302 amplifier discriminator and a Model 9315 ion counter. The discriminator accepts only those pulses with dc levels above the preset discriminator level. Pulses not attenuated by the discriminator are then amplified (×20) before they are counted with the ion counter. A high pass filter with a cutoff frequency of 300 Hz has been added to the system to eliminate low frequency noise (e.g. 60 Hz cycle noise) from the experiment.

For the purposes of this paper the important differences in the experimental procedures from earlier publications are associated with ion formation. Ions are produced in an fast-atom bombardment (FAB) source with an Ion Tech 11-NF fast-atom saddle field gun. Neutral beam densities are estimated from the ion current measured at the cathode of the FAB gun. Although the efficiency for neutralization of the Ar^+ (or Xe^+) beam is not known, the density of the Ar (or Xe) neutral beam is proportional to the measured cathode ion current. The gas line to the FAB gun has been modified by addition of a "normally closed" pulsed valve (General Valve Corp., Model 9-89-900), which is used to control the gas flow to the FAB gun. In a typical pulsed FAB experiment, the metering valve that controls gas flow to the FAB gun for continuous mode operation is completely opened, and gas flow is controlled by the pulsed valve. To perform continuous FAB experiments, the pulsed valve is set to the "open" position and gas flow is controlled by the metering valve.

In the experiments described in the following section the FAB gun high voltage is adjusted to 6–7 kV, and a volume of gas is admitted to the FAB gun by a 5-ms pulse applied to the pulsed valve. At the critical pressure of neutral gas, voltage breakdown produces a short duration fast-neutral beam. The neutral beam densities (100–150 μA; as measured on the source control unit)

are much greater than those used for continuous FAB experiments (10–20 μA). The high neutral beam densities used in the pulsed FAB mode have no deleterious effect upon the operation of the FAB gun. In addition, sample/matrix degradation is reduced and sample lifetimes on the probe tip are extended to hours. For example, with an ion source region background pressure of 10^{-5} Torr (effective pumping speed of 160 L/min), conditions comparable to Ar FAB, 1 microliter of glycerol placed on the FAB probe and inserted into the ion source and removed for inspection at 30-min intervals remains as a visible droplet for greater than 4 h. Conversely, a 1-μL droplet of glycerol (all other conditions unchanged) bombarded with an Ar neutral beam (ca. 10 μA, as indicated by the cathode ion current) ceases to yield glycerol monomer and cluster ions after approximately 20 min.

Collision-induced dissociation measurements were performed by using He target gas to pressurize the activation cell positioned in the third field free region of the mass spectrometer. Crossed-beam photodissociation measurements were performed by using the 488-nm line of an argon ion laser (Coherent Model CR-18).

Dinitrophenyl (DNP) derivatized peptides were purchased from Chemical Dynamics Corp. (South Plainfield, NJ), and nitrobenzyl alcohol, glycerol, and methanol were purchased from Aldrich Chemical Co., (Milwaukee, WI). Solutions of each peptide were prepared by dissolving 1 mg of each peptide into 10 mL of HPLC grade methanol. Approximately 1 μL of the solution was placed on the FAB probe and mixed with 1 μL of FAB matrix (nitrobenzyl alcohol). Because no measurable impurities were observed in the mass spectra of these compounds, the samples were used without purification.

RESULTS AND DISCUSSION

This work compares and quantifies the total ion yields for pulsed and continuous FAB ionization for several small peptides and glycerol clusters. These studies were performed on a triple sector tandem mass spectrometer equipped with ion counting detection and a standard Kratos FAB ion source modified to perform pulsed ionization. Although this experimental apparatus is excellent for many types of experiments, it is somewhat limited for pulsed ionization. The principal disadvantage of the experimental apparatus operating in the pulsed ionization mode is that only a very narrow mass range can be monitored (e.g. peak maxima) for each ionization pulse. This limitation arises because the maximum repetition rate for ion production is 5 s. At higher repetition rates, excessive pressures in the ion source attenuate the ion currents (see Experimental Section). Because well-defined peak profiles using an ion-beam instrument require an ion intensity measurement every 10^{-2}–10^{-3} mass units, a full mass spectrum for a 500 molecular weight sample would require excessively long data acquisition times (i.e. 69–694 h). Therefore, to demonstrate the enhancement in sensitivities using a pulsed ion source, the results reported are obtained by monitoring the ion count rate at the particular mass-to-charge ratio. The peak maxima are located by using continuous FAB ionization, and the instrument is tuned to optimize the ion signal. No additional instrument tuning is used to optimize the pulsed ionization signal.

The $[M + H]^+$ ion yield for the protected (dinitrophenyl (DNP)) hexapeptide DNP-Leu-Gly-Ile-Ala-Gly-Arg-amide (m/z 752) by continuous and pulsed Xe FAB are presented in Figure 1. Xe neutral beam densities of 20 and 100 μA were used for the continuous and pulsed modes, respectively. With pulsed FAB ionization, there is a 100-ms delay time between opening the pulse valve and detecting ions at the electron multiplier of the mass spectrometer. The 100-ms delay corresponds to the time required to reach the critical pressure within the FAB gun to produce a gas discharge plus the ion flight time from the ion source to the detector. [Note, the ion flight time in an ion-beam mass spectrometer is negligible (20–60 μs) compared to the observed delay time.] The same 100-ms delay time is observed for both Ar and Xe FAB gases.

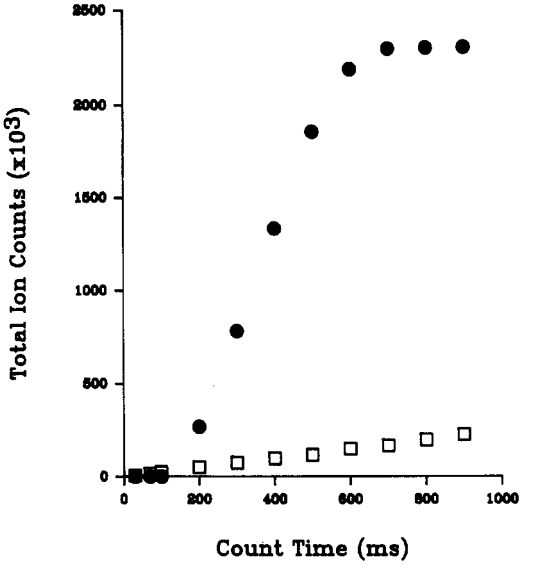

Figure 1. Comparison of the total ion yields for continuous and pulsed Xe FAB as a function of count time for the production of DNP-leucyl-glycyl-isoleucyl-alanyl-glycyl-arginine amide H^+ (m/z 752): (●) pulsed ionization; (□) continuous ionization.

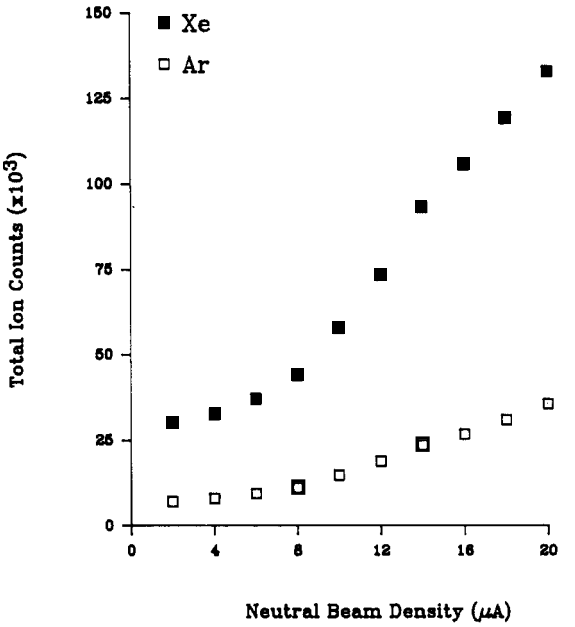

Figure 2. Total ion yields as a function of neutral beam density for the production of DNP-glycyl-valine H^+ (m/z 341) by continuous FAB.

In the remaining pulsed FAB studies reported herein, ion counting was not started until 100 ms following the actuation of the pulse valve, thereby allowing direct comparisons to be made between continuous and pulsed FAB ionization.

Although the pulsed valve is opened for just 5 ms, the data in Figure 1 suggest that ion production occurs over a period of several hundred milliseconds. The duration of ion production directly reflects the pressure profile of the pulsed gas load and the duration of discharge of the fast neutral gun. Note that 90% of the ion signal is formed within 500 ms of the pulsed valve opening, and at times ≥600 ms no additional molecular ions are produced. The maximum advantage of pulsed FAB occurs 400 ms after the onset for ion production (500 ms count time–100 ms dead time) where the measured ion count is approximately 16 times that of continuous FAB.

Figure 2 contains a plot of the relative yields for $[M + H]^+$ ions of dinitrophenyl-glycyl-valine as a function of the neutral beam density by continuous FAB ionization. Ion count measurements were made for neutral beam densities ranging

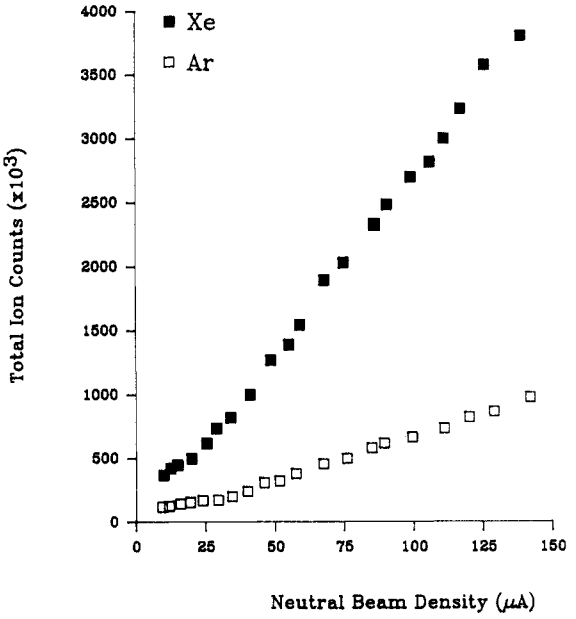

Figure 3. Total ion yields as a function of neutral beam density for the production of DNP-glycyl-valine H^+ (m/z 341) by pulsed FAB.

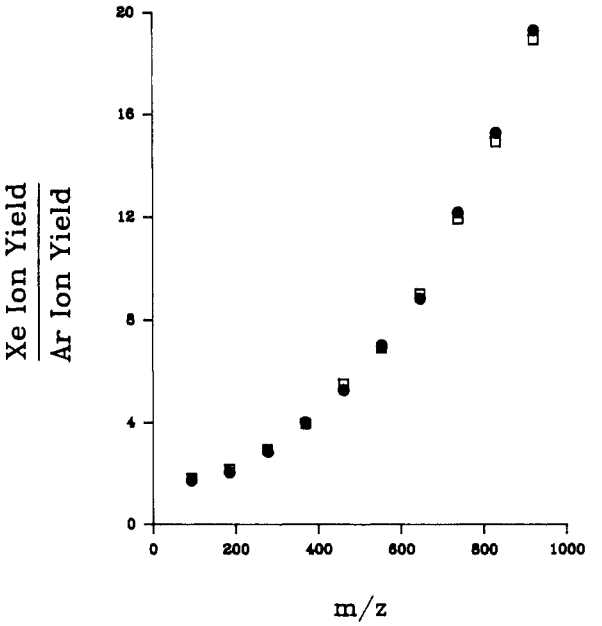

Figure 4. Ratio of total ion yields for Ar and Xe FAB as a function of the mass-to-charge ratio for the glycerol cluster ions, $(G)_nH^+$, n = 1–10: (●) pulsed ionization; (□) continuous ionization.

from 2 to 20 μA by using both 6-keV argon and xenon neutral primary beams. The total ion count times used in these measurements was reduced to 1 ms to avoid overfilling the count registers of the ion counter (i.e., maximum number ion counts = 9.99×10^6 per counting cycle). At the highest neutral beam density (20 μA) used, Xe bombardment produces approximately 130×10^3 ions, and the ion yield for Ar FAB is approximately 36×10^3.

Figure 3 contains a plot of the relative yields for the $[M + H]^+$ ion of dinitrophenyl-glycyl-valine as a function of the neutral beam density by pulsed FAB ionization. At the maximum neutral beam density used in the pulsed FAB experiment (142 μA), Xe and Ar bombardment produces approximately 25 times the number of ions measured in the continuous FAB experiment ($\sim 4 \times 10^6$ and 1×10^6 counts, respectively). It is interesting to note that at low neutral beam densities where direct comparisons between continuous and pulsed FAB can be made (≤20 μA), the sputtered ion yield for the pulsed mode is approximately 4 times that for continuous ionization. This result implies that there is an inherent 4× gain for pulsed over continuous FAB ionization. The increased yield for $[M + H]^+$ ions could be influenced by the solvent dynamics of the liquid matrix or due to reductions in probabilities for collision-induced dissociation and neutralization reactions (*15*). Experiments designed to probe this question further are now under way.

The ratio of total ion yields for Xe and Ar FAB is found to remain fairly constant for both the continuous (3.7–4.0) and pulsed (3.6–4.2) modes (see Figures 2 and 3). However, this ratio is very sensitive to the mass of the desorbed ion. For example, Figure 4 compares the ion yields for xenon and argon FAB as a function of the mass-to-charge ratio for the glycerol cluster ions, e.g. $(G)_nH^+$, n = 1–10. The ratio of ion yields varies from 1.8 at m/z 93 to ~20 at m/z 921. Note that the ratio does not change significantly between pulsed and continuous FAB. Likewise, the ratio for $[M + H]^+/[S + H]^+$ (M = sample and S = matrix) does not vary significantly between pulsed and continuous FAB. For example, when M = DNP-Gly-Val and S = nitrobenzyl alcohol, the ratio $[M + H]^+/[S + H]^+$ is found to be 0.89 and 0.84 for pulsed and continuous FAB modes, respectively. Likewise, when M = DNP-Pro-Leu-Gly and S = nitrobenzyl alcohol, the $[M + H]^+/[S + H]^+$ ratio is 0.40 and 0.42 for pulsed and continuous FAB ionization, respectively. These results indicate that the enhancements in pulsed FAB versus continuous FAB are not due to preferential ionization of the sample over the matrix but instead result from overall increase in the numbers of ions that are produced.

Tables I–III compare the yields for CID product ions and photofragment ions for pulsed and continuous FAB ionization. The samples used for these studies are dinitrophenyl (DNP) derivatized peptides. The DNP-peptides were chosen because the DNP group is a good chromophore for the blue-green wavelength region of the argon ion laser (*18*). The choice of collision-induced dissociation and photodissociation reaction channels to monitor were made on the basis of signal intensity and the presence of background signal (i.e., chemical noise). Because the major source of noise in the photodissociation experiment arises from metastable background signals (*19*), we chose to monitor CID and photodissociation reactions that have appreciable metastable background. Thus, the signal-to-noise ratio for the various signals is directly dependent upon the extent to which the background signals can be removed. In a separate paper we have described how an Einsel lens assembly can be used to reduce the magnitude of the metastable ion background (*19*). In terms of comparing the relative abundance of CID fragment ions there are problems associated with studying CID product ions which are also observed in the metastable ion spectrum (*20*). However, because we are only interested in making comparisons in CID or photofragment ion yields for the two ionization modes, the presence of both metastable ion and CID (or photofragment ion) signals is of no consequence for the present study.

Table I lists the relative CID product ion yields (400 ms count time) for the loss of the glycine residue (B_2 cleavage reaction, structure I) from the $[M + H]^+$ ion of DNP-prolyl-leucyl-glycine by continuous and pulsed FAB ionization. The B_2 cleavage reaction accounts for ca. 17% of the total CID product ion yield (*18*). Collisional activation was performed by passing the 8-keV $[M + H]^+$ ions through an activation cell containing He at a pressure corresponding to 25% attenuation of the main beam. Fifteen individual measurements of the ion counts were made both with and without the presence of target gas in the activation cell. The average of the 15 measurements is reported in Tables I–III. The CID signal is obtained by substracting the metastable background counts (gas off) from the metastable background + colli-

Table I. Relative Collision-Induced Dissociation Yields for the Loss of the Glycine Residue from the $[M + H]^+$ Ion of DNP-Prolyl-Leucyl-Glycine (m/z 452) by Continuous and Pulsed FAB Ionization

Continuous Fast-Atom Bombardment

	gas on	gas off
	22613	18277
	22786	18103
	22665	18190
	22587	18003
	22696	17928
	22538	17873
	22405	17952
	22482	18040
	22761	18260
	22437	17998
	22790	17887
	22411	18156
	22604	18081
	22541	18045
	22451	18005
$\bar{x}$ =	22584 ± 134	18053 ± 125

gas on − gas off = 4500 ± 200

Pulsed Fast-Atom Bombardment

	gas on	gas off
	381675	311229
	381201	312587
	380847	311989
	381229	311370
	382018	311265
	380890	311841
	381424	310425
	380909	311080
	380857	312115
	380872	312311
	381658	311373
	381756	312052
	381260	311836
	381079	312409
	379252	312266
$\bar{x}$ =	381128 ± 640	311743 ± 598

gas on − gas off = 69000 ± 1000

sion-induced dissociation signal counts (gas on). For continuous FAB the CID signal is measured to be 4500 ± 200 counts, whereas pulsed FAB yields 69000 ± 1000 counts. The CID signals obtained by using pulsed FAB are 15 times larger than those for continuous FAB. Note that the ratios for the CID yields from the pulsed and continuous ionization are comparable to the gains measured for total ion yields of DNP-glycyl-valine in Figures 4 and 5. We estimate that the efficiency for CID of the DNP-prolyl-leucyl-glycine $[M + H]^+$ ions is approximately 1 in 450 (0.2%) ions. Note that the uncertainty (±1000 counts or 1.5%) in the measured CID signals in Table I is small relative to signal magnitude (69000).

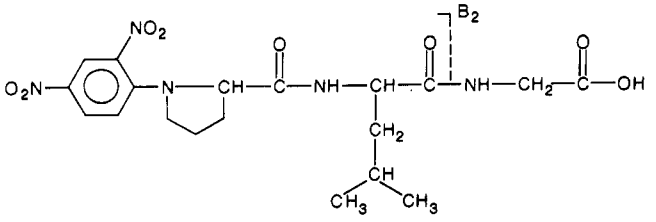

I

Table II lists the relative photodissociation yields (λ = 488 nm) for loss of CO-valine (A_1 cleavage reaction, structure II)

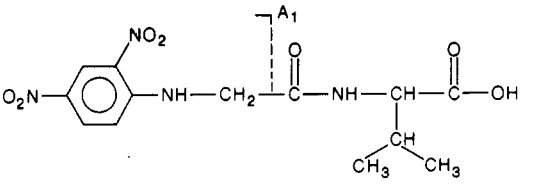

II

from the $[M + H]^+$ ion of DNP-glycyl-valine for continuous and pulsed FAB ionization. On the basis of previous studies we know that the photodissociation cross section for the A_1 cleavage reaction is typical of small organic ions (i.e., m/z <300). The photodissociation signal obtained by pulsed FAB ionization is 34000 ± 2000, whereas the photodissociation signal for the same reaction channel by continuous FAB is 1200 ± 400 counts. Thus a gain of about 28 is obtained for pulsed FAB. The efficiency for producing photofragment ions can be estimated from the difference in the laser "on" and laser "off" signals and the main beam signals. For example, the $[M + H]^+$ ion signal for DNP-glycyl-valine is 2.4×10^7 counts/s and the A_1 photofragment ion yield is approximately 1200 counts/s. Thus, we estimate that 0.005% (1/20000) of the $[M + H]^+$ ions of DNP-glycyl-valine undergo photodissociation. Although the total ion yields for continuous and pulsed FAB are different, the fraction of ions that photodissociate does not vary significantly.

Measurements of weak photodissociation signals superimposed on a large metastable ion background are very difficult because the signal fluctuates randomly above and below the background noise. In cases where continuous FAB produces photodissociation signals just at this noise level, high gains by pulsed FAB can be achieved. For example, Table III lists the relative photodissociation yields (λ = 488 nm) for the B_2 cleavage reaction (I) of the $[M + H]^+$ ion of DNP-prolyl-leucyl-glycine for continuous and pulsed FAB ionization. The photodissociation signal for continuous FAB ionization is 20 counts with a maximum uncertainty of ±200 counts. Because the uncertainty in the continuous FAB photodissociation signal exceeds the measured difference signal, no appreciable photodissociation signal is observed. The negligible difference in ion counts between laser "on" and laser "off" results from the extremely low photodissociation cross section for this transition (the photodissociation efficiency is 1 in 140,000; estimate made by comparing laser "on" versus laser "off" signals, $[M + H]^+$ ion count rate of 2.7×10^6). However, measurements of the photodissociation signal are further complicated by the presence of background metastable signal. Conversely, the photodissociation signal obtained by using pulsed FAB is 1200 ± 800. Thus, pulsed FAB ionization results in increased sensitivities which allow particulary weak signals to be measured with reduced data collection times. Note, however, that the uncertainty in the signal is appreciable (±800 counts) relative to the ion signal (1200 counts). Therefore, in this case it would certainly be desirable to eliminate or reduce the amount of metastable ion signal. The metastable background can be reduced by a factor of 20 by using a biased activation cell (*19*). Use of the biased activation cell reduces the uncertainity in the photodissociation signal for the B_2 cleavage reaction of DNP-prolyl-leucine-glycine $[M + H]^+$ ions accordingly, e.g., 1200 ± 40 counts or an uncertainity for the photodissociation signal of 3.3%.

CONCLUSIONS

In addition to increasing sample lifetimes, pulsed FAB results in enhancements in the total ion yields, as well as the ion yields for collision-induced dissociation and photodissociation. This is a result of higher ion survival rates (due to lower source region pressures) and the higher primary neutral

Table II. Relative Photofragment Ion Yields for Loss of CO-Valine from the $[M + H]^+$ Ion of DNP-Glycyl-Valine (m/z 341) for Continuous and Pulsed Xe FAB Ionization

Continuous Fast-Atom Bombardment

	laser on	laser off
	65 557	64 689
	65 436	64 592
	65 307	64 761
	65 708	63 905
	65 266	64 435
	65 493	64 289
	65 999	64 065
	65 319	64 328
	65 645	64 292
	66 065	64 490
	65 320	64 308
	66 068	64 487
	65 627	64 376
	65 658	64 247
	65 679	64 551
$\bar{x}$ =	65 610 ± 269	64 388 ± 225

laser on − laser off = 1200 ± 400

Pulsed Fast-Atom Bombardment

	laser on	laser off
	1 212 708	1 179 148
	1 211 461	1 176 997
	1 213 121	1 179 649
	1 214 994	1 177 331
	1 212 659	1 179 397
	1 214 856	1 176 931
	1 212 776	1 178 312
	1 211 716	1 176 802
	1 211 433	1 177 083
	1 213 178	1 179 169
	1 212 981	1 180 086
	1 212 503	1 178 225
	1 213 566	1 178 037
	1 211 930	1 178 254
	1 211 028	1 179 185
$\bar{x}$ =	1 212 727 ± 1155	1 178 307 ± 1095

laser on − laser off = 34 000 ± 2000

Table III. Relative Photofragment Ion Yields for Loss of the Glycine Residue from the $[M + H]^+$ Ion of DNP-Prolyl-Leucyl-Glycine (m/z 452) for Continuous and Pulsed Xe FAB Ionization

Continuous Fast-Atom Bombardment

	laser on	laser off
	18 392	18 450
	18 136	18 465
	18 259	18 408
	18 483	18 090
	18 243	18 323
	18 302	18 059
	18 169	18 287
	18 113	18 212
	18 486	18 279
	18 284	18 227
	18 447	18 173
	18 492	18 419
	18 327	18 407
	18 115	18 424
	18 439	18 107
$\bar{x}$ =	18 313 ± 139	18 293 ± 144

laser on − laser off = 20 ± 200

Pulsed Fast-Atom Bombardment

	laser on	laser off
	301 187	300 230
	301 439	300 357
	300 998	299 331
	300 434	300 345
	299 862	299 907
	300 829	299 878
	301 396	299 768
	301 291	300 082
	301 382	300 240
	301 676	299 209
	301 835	299 216
	301 317	300 529
	301 820	301 185
	301 492	300 344
	301 848	300 293
$\bar{x}$ =	301 254 ± 547	300 061 ± 532

laser on − laser off = 1200 ± 800

beam densities that are obtainable in the pulsed FAB experiment. The smaller pulse widths, negligible gas loads, and increased repetition rates of a pulsed Cs^+ ion gun are expected to afford even higher sensitivites than the pulsed FAB experiment presented herein. The enhanced sensitivities obtained by the pulsed FAB source are particularly important for high mass/high resolution applications where ion beam currents are typically very small (i.e. $<10^{-14}$ A). The ion bunching effect that results from pulsing the primary ion or neutral beam is more amenable to photodissociation MS–MS than for collision-induced dissociation MS-MS. The primary advantage of pulsing the ion beam for photodissociation experiments is that a high-intensity photon beam can be synchronized to the arrival time of the ion packet. One application that should prove fruitful is combining the pulsed ion beam technique with high-power pulsed lasers for performing photodissociation. Unlike the continuous laser used in the present studies, pulsed lasers, e.g., the Nd^{3+} YAG and excimer lasers, offer extremely high peak powers (typically $>10^8$ W/cm^2) for short periods of time ($\sim$10 ns) and at relatively low repetition rates. The combined high laser powers and high ion densities obtainable in pulsed ion source pulsed laser experiments are expected to afford large (approaching unity) photodissociation efficiencies (primary ions → photofragment ions). Hence, the laser-ion beam photodissociation of large biomolecules could prove to be a viable analytical method for structural characterization.

The combined use of pulsed ion sources with ion-beam mass spectrometers is currently limited to monitoring narrow mass windows within the mass spectrum. This limitation can be overcome, however, by using an array detector (*21*) with double-focusing ion-beam instruments (*22*, *23*). Ion-beam mass spectrometers with array detectors allow all masses in a large mass range issuing from the magnetic analyzer to be focused on to a single flat plane. If an array detector is positioned in this plane, large portions of the full mass spectrum can be acquired nearly simultaneously. Hence, it is reasonable to suspect that full MS–MS spectra with increased sensitivities and reduced data collection times could be collected for moderately small ion signals ($\sim 10^{-13}$ A) with 5–10 pulses of the primary ion source. In our laboratory we are developing a tandem magnetic sector/time-of-flight laser photodissociation apparatus for analyzing clusters and biomolecules. This instrument concept is ideally suited for pulsed ionization-pulsed photodissociation experiments and we project a sensitivity increase of 300 times that of the current laser-ion beam photodissociation apparatus (*24*).

LITERATURE CITED

(1) Barber, M.; Bordoli, R. S.; Elliott, G. J.; Sedgwick, R. D.; Tyler, A. N. *Anal. Chem.* **1982**, *54*, 645A.

(2) Williams, D. H.; Bradley, C.; Bojesen, G.; Santikarn, S.; Taylor, L. C. E. *J. Am. Chem. Soc.* **1981**, *103*, 5700.
(3) Burlingame, A. L.; Baillie, T. A.; Derrick, P. J. *Anal. Chem.* **1986**, *58*, 165R.
(4) Burlingame, A. L.; Russell, D. H.; Maltby, D.; Holland, P. T. *Anal. Chem.* **1988**, *60*, 294R.
(5) Tomer, K. B.; Crow, F. W.; Gross, M. L.; Kopple, K. D. *Anal. Chem.* **1984**, *56*, 880.
(6) Amster, I. J.; McLafferty, F. W. *Anal. Chem.* **1985**, *57*, 1208.
(7) Cotter, R. J.; Larsen, B. S.; Heller, D. N.; Campana, J. E.; Fenselau, C. *Anal. Chem.* **1985**, *57*, 1479.
(8) Biemann, K.; Martin, S. A. *Mass Spectrom. Rev.* **1987**, *6*, 1.
(9) Jensen, N. J.; Gross, M. L. *Mass Spectrom. Rev.* **1987**, *7*, 1.
(10) Long, G. L.; Winefordner, J. D. *Anal. Chem.* **1983**, *55*, 712A.
(11) Caprioli, R. M.; Fan, T.; Cottrell, J. S. *Anal. Chem.* **1986**, *58*, 2949.
(12) Hunt, D. F.; Shabanowitz, J.; Yates III, J. R.; Zhu, N. Z.; Russell, D. H.; Castro, M. E. *Proc. Natl. Acad. Sci. U.S.A.* **1987**, *84*, 620.
(13) Russell, D. H. *Mass Spectrom. Rev.* **1986**, *5*, 167.
(14) Aberth, W.; Straub, K. M.; Burlingame, A. L. *Anal. Chem.* **1982**, *54*, 2029.
(15) Aberth, W. *Anal. Chem.* **1986**, *58*, 1221.
(16) Olthoff, J. K.; Cotter, R. J. *Nucl. Instrum. Methods Phys. Res., Sect. B* **1987**, *B26*, 566.
(17) Tecklenburg, R. E., Jr.; Russell, D. H. *J. Am. Chem. Soc.* **1987**, *109*, 7654.
(18) Tecklenburg, R. E., Jr.; Miller, M. N.; Russell, D. H. *J. Am. Chem. Soc.*, in press.
(19) Tecklenburg, R. E., Jr.; Sellers-Hann, L.; Russell, D. H. *Int. J. Mass Spectrom. Ion Proc.*, in press.
(20) Cooks, R. G. *Collision Spectroscopy*; Cooks, R. G., Ed.; Plenum Press: New York, 1978; pp 405–406.
(21) Ashcroft, A. E.; Brown, R. S.; Coles, A. D.; Evans, S.; Milton, D. J.; Wright, B. *Spectroscopy* **1987**, *3*, 57.
(22) Ouwerkerk, C. E. D.; Boerboom, A. J. H.; Matsuo, T.; Sakurai, T. *Int. J. Mass Spectrom. Ion Processes*, **1986**, *70*, 79.
(23) Zhaoheng, H.; Chen, H.; Boerboom, A. J. H.; Matsuda, H. *Int. J. Mass Spectrom. Ion Processes* **1986**, *71*, 29.
(24) Tecklenburg, R. E., Ph. D. Thesis, Texas A&M University, 1988.

RECEIVED for review May 23, 1988. Accepted October 18, 1988. This work was supported by grants from the U.S. Department of Energy, Office of Basic Energy Sciences (DE-AS05-82ER13023) and the National Science Foundation (CHE-8418457).

Microhole Array for Oxygen Electrode

Ken-ichi Morita*[1] and Yoshihiro Shimizu

Basic Research Laboratories, Toray Ind., Inc., 1111 Tebiro, Kamakura-shi, Kanagawa-ken, 248 Japan

Carbon fiber–epoxy composite ultramicroelectrode arrays were etched to depths of several hundred micrometers to create an array of microholes of the diameter of the carbon fiber (4–7 μm). The cylindrical wells that form over active microdisk electrodes (platinized carbon fiber) reimpose linear diffusion to each microelectrode. A solid-state polarographic oxygen sensor was fabricated by using the microhole array. For the assembled arrays the thickness of the diffusion layer for the reduction of dissolved oxygen was found to be the sum of the depth of the microhole and the thickness of the solution boundary layer. The ultramicrohole/microelectrode array has the advantages of being moderately flow-rate-insensitive and discriminative against macromolecular poisons.

Recently, microelectrodes less than 7 μm in radius have become readily available because of progress in carbon fiber technology (*1*). They exhibit several striking features that have facilitated their use in electrochemical studies (*2–7*). The concept of a microhole array with the resulting cylindrical well controlling diffusion has been demonstrated (*8*, *9*). The recessed electrode has been examined (*10–13*) for potential use as a polarographic oxygen sensor.

Recessed ultramicroelectrode arrays are produced by oxidative etching of polished sections of carbon fiber–epoxy composites, followed by plating with platinum. Scanning electron micrographs of the surface of the microhole electrode and a cross-sectioned view of a microhole showing the platinized carbon fiber are shown in Figure 1. The solution well over a microdisk electrode is protected from convection in the bulk fluid and acts as a diffusion layer in the electrochemical process. Compared to a bare electrode, the electrodes are far less sensitive to changes in thickness of the boundary layer (outer diffusion layer) on the surface of the probe caused by a flow of liquid. It is also important from a practical viewpoint to note that microholes behave as a filter that prevents electrode contamination and pollution. Dissolved oxygen sensors made from microhole electrode arrays showed several advantages over a conventional Clark-type sensor.

EXPERIMENTAL SECTION

Fabrication of Microhole Electrodes. High-tensile-strength carbon fibers were used (heat-treated at 1300–1500 °C, the number of fibers ranging from 1000 to 6000 filaments). High modulus carbon fibers (heat-treated over 2000 °C) resisted oxidative etching. A bundle of 1000 filaments of high-strength carbon fibers (Torayca T-300, 1 K, diameter 6.93 μm) was pulled through a resin bath of polymeric binder material consisting of 97 parts of epoxy (Chissonox 221, Yuka Shell, Tokyo, unless otherwise stated) to 3 parts of BF_3-monoethylamine, and the resin-impregnated fibers were wound onto a wooden spool. The impregnated yarn was then cured in an air-heated dryer at 130 °C for 30 min. A needle-type composite was obtained. Various types of carbon fibers were treated in the same way (Table I). Diameters of the microelectrode arrays were 0.3 mm for 1000 pieces of fiber and 0.8 mm for 6000 pieces of fiber. The electrode was prepared by placing the composite in a polyethylene tube with an inside diameter of 2 mm and drawning an epoxy resin into the tube. After curing, the rod was removed from the tube and cut into sections about 10 cm long. One end of the rod was ground with sandpaper (2000 grit), and an electrical lead was bonded to it with a conductive silver paste (Dotite D-435, Fuzikura Kasei). The other end was polished to a mirror finish by using a 12-μm lapping film followed by a 0.3-μm lapping film using Handy Fiber Polisher, Type OFL-4 (Seiko Instruments & Electronics, Ltd). After being polished, the rod was rinsed with deionized water and carefully wiped. The mirror section was immersed in a 2 mM sulfuric acid solution containing 0.2 M sodium sulfate and anodically etched at a constant current greater than 800 mA/cm^2. The depth of etching was nearly proportional to the amount of charge added, and the limit of etching was about 500 μm. The depths of the microholes were measured by an optical microscope or a scanning electron

[1] Present address: Tōin University of Yokohama, 1614 Kurogane-cho, Midori-ku, Yokohama, Kanagawa-ken, 227 Japan.

0003-2700/89/0361-0159$01.50/0